Intensity Ratios of $I_{L\beta}/I_{L\alpha}$ and $I_{L\gamma}/I_{L\alpha}$: Semi-Theoretical Formulae for Diverse Elements under Photon Excitation with 1.9 keV < E_{inc} ≤ 200 keV

A. Zidi[1,2], A. Kahoul[1,2*], J.P. Marques[3,4], K. Amari[1,2], S.Daoudi[1,2], J.M. Sampaio[3,4], F. Parente[5], A. Hamidani[1,2], S. Croft[6], A.Favalli[7,8], Y. Kasri[9,10], B. Berkani[1,2]

[1]*Department of Matter Sciences, Faculty of Sciences and Technology, Mohamed El Bachir El Ibrahimi University, Bordj-Bou-Arreridj 34030, Algeria.*
[2]*Laboratory of Materials Physics, Radiation and Nanostructures (LPMRN), Faculty of Sciences and Technology, Mohamed El Bachir El Ibrahimi University, Bordj-Bou-Arreridj 34030, Algeria.*
[3]*LIP – Laboratório de Instrumentação e Física Experimental de Partículas, Av. Prof. Gama Pinto 2, 1649-003 Lisboa, Portugal.*
[4]*Faculdade de Ciências da Universidade de Lisboa, Campo Grande, C8, 1749-016 Lisboa, Portugal.*
[5]*Laboratory of Instrumentation, Biomedical Engineering and Radiation Physics (LIBPhys-UNL), Department of Physics, NOVA School of Science and Technology, NOVA University Lisbon, 2829-516 Caparica, Portugal.*
[6]*School of Engineering, Faculty of Science of Technology, Nuclear Science & Engineering Research Group, Lancaster University, Bailrigg, Lancaster, LA1 4YW, United Kingdom.*
[7]*European Commission, Joint Research Centre, Ispra, I-21027, Italy.*
[8]*Los Alamos National Laboratory, P.O. Box 1663, Los Alamos, NM 87545, USA.*
[9]*Physics Department, Faculty of Sciences, University of Mohamed Boudiaf, 28000 M'sila, Algeria.*
[10]*Theoretical Physics Laboratory, Faculty of Exact Sciences, Bejaia University, 06000 Bejaia, Algeria.*

[*]Corresponding author. Tel. /Fax (+213) 035862230.
E-mail address: *a.kahoul@univ-bba.dz ; ahalim.kahoul@gmail.com*

Abstract: The main objective of this paper is to calculate semi-theoretical values for the L-shell X-ray intensity ratios $I_{Li}/I_{L\alpha}$ (i= β and γ) across a broad range of elements in the atomic number range 36 ≤ Z ≤ 92 and photon excitation energies spanning from 1.916 keV to 200 keV. These values are derived from theoretical calculations and subsequently refined using an advanced interpolation approach based on a three-dimensional function incorporating atomic number Z and excitation energy E. The dependence of the L-shell intensity ratios on the incident photon energy is analyzed, highlighting variations across different elements. A comparison was carried out for selected excitation energies of 22.6 keV and 59.54 keV, integrating weighted average values, theoretical calculation, and experimental data from the literature to evaluate their reliability and accuracy.

Keywords: X-ray fluorescence, intensity ratios, semi-theoretical calculation, and weighted average values.

1. Introduction

Atomic parameters are essential data for various basic and applied scientific fields, including atomic physics and medical research, as they provide critical insights into the behavior of matter at the atomic level and how radiation interacts with matter. Among these parameters, fluorescence yields indicate the efficacy with which absorbed energy is converted into emitted X-rays. Fluorescence cross-sections play a pivotal role in determining the yield of emitted X-rays and are intimately related to the interaction of incident photons with atomic structures. Furthermore, the study of intensity ratios is vital for understanding the relative contributions of different X-ray emission processes. Vacancy-transfer probabilities also significantly affect intensity ratios, influencing how efficiently energy is transferred between electron states. Additionally, the jump factors, which describe the abrupt changes in atomic parameters due vacancy filling, are crucial for refining intensity ratios, especially within the framework of multi-electron transitions and their impact on X-ray emission. In this context, several studies have introduced advanced techniques for empirical and semi-empirical calculations of these atomic parameters. For instance, Amari *et al.* [1] employed a three-dimensional interpolation method to accurately calculate empirical K-shell X-ray fluorescence cross-sections for photon energies ranging from 5.46 keV to 123.6 keV. In the same year, Berkani *et al*. [2] calculated empirical values based on a database of vacancy transfer probabilities for elements with atomic numbers from Z=16 to 92. In addition, semi-empirical $I_{K\beta}/I_{K\alpha}$ intensity ratios for elements with $11 \leq Z \leq 96$ were calculated by Hamidani *et al.* [3]. Notably, Meddouh *et al.* [4] performed semi-empirical evaluations of fluorescence yields for the K-shell in elements with atomic numbers Z= 14 to 99, the L-shell for Z= 23 to 96, and the M-shell for Z= 40 to 92. For more comprehensive insights into the empirical and semi-empirical calculations of atomic parameters, the works of various authors can be consulted [5-7]. In contrast to these calculations, the jump factors have been experimentally determined in the studies by Cengiz *et al.* [8,9]. Other atomic parameters have also been obtained experimentally, for example, fluorescence parameters of thallium in thallium compounds were determined by Cengiz *et al.* [10]. These experimental investigations contributed significantly to the comprehensive understanding of X-ray emission processes and their dependency on atomic structure. This study specifically focuses on L-shell X-ray intensity ratios, a parameter extensively explored in support of wide-ranging applications.

Many researchers and research teams have experimentally determined the values of the intensity ratios of X-ray emission from the L-shell for all periodic table elements, using different sources and detectors. Garg *et al*. [11] measured the $I_{L\beta}/I_{L\alpha}$ and $I_{L\gamma}/I_{L\alpha}$ intensity ratios for $_{67}$Ho, $_{68}$Er, and $_{70}$Yb using 22.6 keV photons emitted from a ^{109}Cd source, using a Si (Li) detector. Rao *et al*. [12] employed an X-ray tube with a secondary exciter and germanium detector to determine the $I_{L\beta}/I_{L\alpha}$, $I_{L\gamma}/I_{L\alpha}$, and $I_{Ll}/I_{L\alpha}$ intensity ratios for $_{79}$Au and $_{82}$Pb. Dhal and Padhi [13] measured the same intensity ratios using 59.54 keV γ-rays emitted from a point source of ^{241}Am, and a Si(Li) detector for the elements $_{78}$Pt, $_{82}$Pb, and $_{83}$Bi. The measurement and calculation of L-shell intensity ratios across a wide range of elements have often relied on theoretical models integrated with experimental data and empirical formulae. A least-squares fit was used by Salem *et al.* [14] to analyze the available experimental data plotted against the atomic number *Z*. This approach allowed them to derive the "most probable" values for L X-ray emission rates ($I_{L\alpha1}$, $I_{L\alpha2}$, $I_{L\beta1}$, $I_{L\beta3}$, $I_{L\beta4}$, $I_{L\beta5}$, $I_{L\beta6}$, $I_{L\beta2,15}$, $I_{L\gamma1}$, $I_{L\gamma2}$, $I_{L\gamma3}$, $I_{L\gamma6}$, $I_{L\eta}$, and $I_{Ll}/I_{L\alpha}$) for elements with $26 \leq Z \leq 96$. In the same year, Scofield [15] employed a relativistic Hartree–Slater calculation to establish the total L-shell radiative decay rates and the emission rates for individual X-ray lines across elements within the atomic number range of $5 \leq Z \leq 104$. Furthermore, Scofield [16] gathered Hartree-Fock-model tabulated values to estimate L-shell X-ray emission rates. These rates were computed for a particular group of atoms that exhibit single vacancies in the L-shell for elements across the atomic number range $18 \leq Z \leq 94$. Puri

[17] reported a study where the X-ray relative intensities of L_i subshells (i = 1–3), derived from emission rates using the Dirac-Fock model, undergo a least-squares fitting to atomic number dependent polynomials, spanning the range $30 \leq Z \leq 92$. These fitted values were aimed at integration into software packages tailored for quantitative elemental analysis employing X-ray emission techniques, and other associated applications. The Dirac-Fock model was employed in a study conducted by Kumar *et al*. [18] to compute intensity ratios $I_{Lk}/I_{L\alpha1}$(k = l, η, α_2, β_1, $\beta_{2,15}$, β_3, β_4, $\beta_{5,7}$, β_6, $\beta_{9,10}$, $\gamma_{1,5}$, $\gamma_{6,8}$, $\gamma_{2,3}$, γ_4), and $I_{Lj}/I_{L\alpha}$ (j = β, γ) for elements with $36 \leq Z \leq 92$. Puri [19] investigated the same intensity ratios and $I_{Lj}/I_{L\alpha}$ (j = β, γ) for different incident photon energies, employing calculations based on the Dirac-Fock model. In our recent work, Zidi *et al*. [20] pioneered the creation of a database of L-shell X-ray intensity ratios data. This database gathered information from 83 papers, totaling 2600 values, meticulously arranged in tables. The elements in the dataset fall within the atomic number range of $39 \leq Z \leq 94$ Additionally, a dedicated table shows information about each author, including the sources and detectors used in their studies. Zidi *et al*. [21] computed empirical values for $I_{L\beta}/I_{L\alpha}$, $I_{L\gamma}/I_{L\alpha}$, and $I_{Ll}/I_{L\alpha}$ intensity ratios, by interpolating experimental data from the databases of Zidi *et al*. [20], and also from new theoretical results by using the multiconfiguration Dirac-Fock method (MCDF) for $_{40}$Zr, $_{48}$Cd, $_{50}$Sn, $_{52}$Te, $_{56}$Ba, $_{80}$Hg, $_{83}$Bi, and $_{86}$Rn.

The K-edge is the threshold energy for the ionization of core electrons from the innermost electron shell (K-shell). Below the K-edge, where the incident photon energy is lower than the K-shell binding energy, ionization predominantly involves the L-shell, leading to relatively unstable intensity ratios on incident photon energies and atomic numbers. Above the K-edge, additional ionization mechanisms such as Coster-Kronig transitions and auger processes redistribute vacancies among the L-subshells. This redistribution alters the fluorescence yields and modifies the relative intensities of L-shell transitions, leading to more systematic variations in intensity ratios across elements and photon energies. The energy dependence of the $I_{L\beta}/I_{L\alpha}$

and $I_{L\gamma}/I_{L\alpha}$ intensity ratios, particularly in relation to the K-edge, has been detailed in the work of Kumar *et al*. [18]. These ratios exhibit distinct variations above and below K-edge due to changes in photoionization cross sections and vacancy redistribution mechanisms.

Due to the lack of data for certain elements and incident photon energies in the study by Kumar *et al*. [18], this work aims to provide a more comprehensive analysis by determining semi-theoretical intensity ratios for $I_{L\beta}/I_{L\alpha}$ and $I_{L\gamma}/I_{L\alpha}$ for elements in the range $36 \leq Z \leq 92$ at incident photon energies ranging from 1.916 to 200 keV. This is achieved through analytical function adjustments based on the theoretical data reported by Kumar *et al*. [18], allowing for a continuous and complete dataset over the considered range. A three-dimensional interpolation was performed to account for their dependence on both atomic number and incident photon energy. To further evaluate the accuracy and consistency of the model, a detailed comparative analysis was conducted, specifically considering excitation energies 22.6 keV and 59.54 keV. This involved integrating weighted average values, theoretical calculations, and experimental data from the literature. The results highlight the robustness of the semi-theoretical approach, revealing its ability to accurately predict intensity ratios across a wide range of atomic numbers and photon energies. Moreover, the analysis provides insights into the limitations of current models suggesting potential avenues for future improvements, particularly in the higher energy domain where discrepancies between theoretical and experimental data become more pronounced.

2. Semi-theoretical calculation

Building on the importance of L-shell X-ray intensity ratios in radiation matter interactions, the article by Kumar *et al*. [18], presents a comprehensive theoretical study aimed at evaluating the relative intensity ratios of L X-ray lines emitted by elements with atomic numbers ranging from 36 to 92, for incident energies in the range $\mathrm{E}_{L1} < \mathrm{E}_{inc} \leq 200$ keV. To achieve this, the authors combine photoionization cross-sections calculated using the relativistic Hartree-Fock-Slater model, X-ray emission rates determined by the Dirac-Fock model, and fluorescence yields as well as Coster-Kronig transition probabilities evaluated via the Dirac-Hartree-Slater model. The formalism employed is based on determining the production cross-section of an L-line. A key aspect of the study concerns the effect of the K-edge. For incident energies exceeding the K-shell threshold, additional vacancies, which can account for 80-85% of the total vacancies in the L-shell, significantly alter the relative intensity ratios of L lines, particularly those originating from L_1 and L_2 subshells, leading to abrupt discontinuities in their values. The detailed results, presented in tables and graphs, focus on a complex dependence of these intensity ratios on photon energy and atomic number, with deviations reaching up to 15% depending on whether the theoretical DHS values or the recommended values from Campbell [22,23] are used. In conclusion, this research provides a rigorous theoretical foundation for the quantitative analysis of L X-ray spectra, essential for analytical applications such as EDXRF. It also emphasizes the need to incorporate electron-electron correlation effects and solid-state effects into models while calling for precise experimental measurements to validate and refine these predictions.

In this current work, semi-theoretical values were determined for the two $I_{L\beta}/I_{L\alpha}$ and $I_{L\gamma}/I_{L\alpha}$ intensity ratios based on the theoretical data published by Kumar *et al*. [18]. The theoretical values for each ratio were initially classified according to the K-edge [24], dividing the energy range into two intervals, one for energies below the K-edge and another for energies above this value, for each element. Then, the values were plotted to examine their overall distribution as a function of atomic number Z. Based on this distribution, the atomic number range for each intensity ratio was divided into five distinct intervals ($36 \leq Z \leq 49$; $50 \leq Z \leq 74$; $75 \leq Z \leq 77$; $78 \leq Z \leq 90$; $91 \leq Z \leq 92$) to improve the accuracy of the interpolation. Figs. 1 to 4 illustrate an example of this division for the interval Z = 50-74, showing how the atomic number range is split. Finally, to enhance the fit, a three-dimensional interpolation was implemented, integrating atomic number Z and excitation energy E. The polynomial function utilized for the fitting process is as follows:

$$\left(\frac{I_{Li}}{I_{L\alpha}}\right)_{S-Theo} = f(Z) \times g(\ln(E)) \quad \text{with } i = \beta, \gamma \tag{1}$$

Here, $f(Z)= \sum_{i=0}^{2} a_i Z^i$ and $g(\ln(E)) = \sum_{i=0}^{2} b_i \ln E^i$.

The chosen of the polynomial function for the fitting process is structured as a product of two distinct polynomial terms: one dependent on the atomic number Z and the other on the natural logarithm of the incident photon energy $\ln(E)$. This functional form was selected based on the distribution of the theoretical values, ensuring an accurate representation of the semi-theoretical intensity ratios. The polynomial term $f(Z)$ accounts for the variations in intensity ratios as a function of atomic number, capturing the underlying trends dictated by atomic structure and transition probabilities. Meanwhile, the term $g(\ln(E))$ models the dependence on photon energy, considering the logarithmic relationship often observed in atomic excitation and ionization processes. The multiplication of these two polynomials allows for a more flexible and precise fit by incorporating the combined effects of both parameters, rather than treating them as independent additive contributions. This approach enhances interpolation accuracy by preserving the nonlinearity inherent in the theoretical data and ensuring smooth transitions across different atomic numbers and photon energies. The chosen function effectively balances complexity and accuracy, allowing for a reliable determination of intensity ratios over the studies range.

The fitting coefficients for the two intensity ratios $I_{L\beta}/I_{L\alpha}$ and $I_{L\gamma}/I_{L\alpha}$ in Eq. (1) are provided in Table 1 (below K-edge) and Table 2 (above K-edge).

3. Root-mean-square error (ε_{RMS})

The discrepancy between observed values (theoretical or experimental data) and those predicted by a model, whether semi-empirical or empirical, often prompts the use of the root-mean-square error (ε_{RMS}) as a metric to assess this difference [25].

For every ratio, the aggregate deviation of *N* experimental data, denoted by $(I_{L\beta}/I_{L\alpha})_{Theo}$ and $(I_{L\gamma}/I_{L\alpha})_{Theo}$ from their respective anticipated values $(I_{L\beta}/I_{L\alpha})_{S-Theo}$ and $(I_{L\gamma}/I_{L\alpha})_{S-Theo}$, is presented, as a percentage, with reference to the root-mean-square error. This calculation is done individually for each ratio, and by using formula (1), employing the expression [26]:

$$\varepsilon_{RMS}(\%) = 100 \times \left[\sum_{j=1}^{N} \frac{1}{N}\left(\frac{\chi_{j(Theo)}-\chi_{j(S-Theo)}}{\chi_{j(S-Theo)}}\right)^{2}\right]^{\frac{1}{2}} \tag{2}$$

Here, *N* is the number of theoretical data points, $\chi_{j(Theo)}$ represents the theoretical $I_{Li}/I_{L\alpha}$ (i = β and γ) intensity ratios, and $\chi_{j(S-Theo)}$ designates the semi-theoretical results within this investigation for the intensity ratios of $I_{Li}/I_{L\alpha}$ ($i = \beta$ and γ). The total root-mean-square error for the semi-theoretical results is presented in Table 1 for measurements below the K-edge and in Table 2 for those above the K-edge.

4. Weighted average value

In atomic and X-ray spectroscopy, accurately determining L-shell intensity ratios is crucial for precise elemental analysis. The weighted average provides a robust statistical method to consolidate data from multiple sources, effectively accounting for varying uncertainties inherent in experimental measurements. In the study by Zidi *et al.* [20] a comprehensive database was constructed, comprising more than 2600 experimental values of X-ray intensity ratios under photon effect, published between 1971 and 2022, for elements with atomic number

39 ≤ Z ≤94. For each element, weighted average values of these intensity ratios were calculated, without taking into account incident energies.

In order to analyze the semi-theoretical results and compare them with the values of Zidi *et al.* [20], weighted average values were calculated using the database of Zidi *et al.* [20] for each element and each incident energy separately. In this research, only two specific photon energies, 22.6 keV and 59.54 keV, were selected for comparison to ensure consistency in the analysis. It is important to note that the data obtained by Aylikci *et al.* [24] were excluded from this analysis because of their high dispersion. Also, we have excluded the values given by the authors [27-32], since the intensities $I_{L\alpha}$, $I_{L\beta}$ and $I_{L\gamma}$ were measured for different energies. This approach reinforces the conclusions of Kumar *et al*'s. [18] study.

In this work, the weighted average of L-shell intensity ratios was computed using the following formula [33]:

$$(I_{\mathrm{L}i}/I_{\mathrm{L}\alpha})_W = \frac{1}{\sum_{n=1}^{N} \frac{1}{(\Delta(I_{\mathrm{L}i}/I_{\mathrm{L}\alpha})_{EXP-n})^2}} \cdot \sum_{n=1}^{N} \frac{(I_{\mathrm{L}i}/I_{\mathrm{L}\alpha})_{EXP-n}}{(\Delta(I_{\mathrm{L}i}/I_{\mathrm{L}\alpha})_{EXP-n})^2} \tag{3}$$

In Eq. (3), $(I_{\mathrm{L}i}/I_{\mathrm{L}\alpha})_{EXP-n}$ (here $i = \beta$ and γ) indicates the n^{th} experimental intensity ratio, N represents for the count of experimental data points, $\Delta(I_{\mathrm{L}i}/I_{\mathrm{L}\alpha})_{EXP-n}$ denotes the uncertainty associated with the n^{th} experimental value.

5. Results and discussion

To facilitate a comprehensive comparison between our semi-theoretical intensity ratios $I_{Li}/I_{L\alpha}$ (i = β and γ) with those reported by other researchers, encompassing theoretical and experimental values, we performed a comparison for two specific incident energies: 22.6 keV and 59.54 keV. These energies were chosen because they are commonly used in our database [20] and studies on X-ray intensity ratios, thus allowing a direct and relevant comparison with existing data. The current results for the intensity ratios $I_{L\beta}/I_{L\alpha}$, $I_{L\gamma}/I_{L\alpha}$ are presented in Tables

3-6 and have been graphically represented alongside other results as a function of the atomic number Z in Figs 5, 6, 7, and 8.

The difference is quantified by the relative percentage difference defined by $RD(\%) = |((I_{Li}/I_{L\alpha})_{Theo} - (I_{Li}/I_{L\alpha})_{s-Theo})/(I_{Li}/I_{L\alpha})_{s-Theo}| \times 100$, between our results and those obtained from different references. This approach allows us to quantitatively assess the divergence between our data and those from other studies, ensuring the relevance and reliability of our analysis.

Fig. 5 shows a comparative analysis of the semi-theoretical values of the $I_{L\beta}/I_{L\alpha}$ intensity ratio at an incident energy of 22.6 keV. In Fig. 5 (a), these values are compared with theoretical calculation of Kumar *et al*. [18] and other available experimental values [34-35]. Upon reviewing this figure, several observations can be made. The present semi-theoretical $I_{L\beta}/I_{L\alpha}$ intensity ratio consistently agrees well with the theoretical values reported by Kumar *et al*. [18] for the entire range of elements, exhibiting a relative difference ranging from 0.02% to 2.81%. However, we find notable discrepancies between our semi-theoretical calculation and available experimental values, as depicted in Fig.5 (a). These discrepancies range from 4.39% to 9.05% for Singh *et al*. [34] except for three elements (0.46% for $_{57}$La, 0.69% for $_{59}$Pr, and 0.39% for $_{62}$Sm). The deviation varies from 0.08% to 13.64% according to Kaçal *et al*. [27]. Figure 5(b) illustrates the semi-theoretical $I_{L\beta}/I_{L\alpha}$ intensity ratio and the weighted average values derived from the Zidi *et al*. [20] database. The data are plotted as a function of atomic number Z. For elements in the range $59 \leq Z \leq 71$, the agreement is satisfactory, with relative deviations confined between 0.12% and 9.05%. However, for lower and intermediate Z values, the discrepancies increase progressively, reaching 85.89% for Z=47, indicating a substantial deviation from the weighted average values.

Figure 6 presents, for 59.54 keV incident photon energy, a comparison of our semi-theoretical $I_{L\beta}/I_{L\alpha}$ intensity ratio with theoretical values published by Kumar *et al*. [18] and experimental data from Durak and Özdemir. [36], Han *et al*. [37], and Akman *et al*. [38], as well as weighted average values. This analysis is divided into two parts: Fig. 6 (a), which examines agreement with theoretical and experimental datasets, and Fig. 6 (b), which compares our results with the weighted average values. In Fig. 6 (a) our semi-theoretical results exhibit an excellent agreement with the theoretical calculations of Kumar *et al*. [18], with *RD* ranging from 0.06% to 2.92%. A comparison with the data of Durak and Özdemir. [36] reveals a more pronounced discrepancy for heavy elements, reaching up to 14.4%, while for the lanthanides ($57 \leq Z \leq 72$), the deviations remain an acceptable range of agreement, with deviations ranging from 0.82% to 5.44%. Moreover, agreement with Han *et al*'s data [37] is observed within 1.73%-5.11%, whereas for Akman *et al*. [38], deviations are generally contained within 0.14% to 5.92%, except for $_{70}$Yb (9.60%) and $_{81}$Tl (10.13%), where notable deviations occur. Fig. 6 (b) compares our semi-theoretical values with weighted average values obtained by Zidi *et al*. [20]. A systematic dispersion is evident across the entire atomic number range, with discrepancies reaching 38.08% for *Z*=75, indicating significant deviations in this region.

In what concerns the $I_{L\gamma}/I_{L\alpha}$ intensity ratio, Fig. 7 illustrates its variation against atomic number *Z* at an incident energy of 22.6 keV. Beginning with Fig.7 (a), this comparison includes theoretical values from Kumar *et al*. [18] and experimental data from Singh *et al*. [34] and Kaçal *et al*. [35]. The semi-theoretical findings obtained in this study demonstrate strong agreement with Kumar *et al*'s. [18] theoretical predictions, with deviations spanning from 0% to 4.83% for *Z*=36-92 (except for $_{40}$Zr). Additionally, the semi-theoretical results exhibit good agreement with the experimental data of Kaçal *et al*. [35], with variations within 0.14-7.94% except for $_{76}$Os (13.8%) and $_{78}$Pt (12.28%). However, a noticeable divergence is observed between our semi theoretical $I_{L\gamma}/I_{L\alpha}$ intensity ratio and the experimental estimates of Singh *et* *al*. [34], with *RD* varying in the range of 8.29-27.40%. Turning our attention to Fig. 7 (b), which compares our results with the weighted average values calculated using Equation (3) over the range *Z*=39-92, it is evident that a strong agreement is observed in the intervals $67 \leq Z \leq 74$ and $77 \leq Z \leq 90$. However, for the remaining elements, significant deviations are noted.

The examination of Fig. 8 facilitates the comparison between the theoretical findings of Kumar *et al*. [18], experimental values in Fig.8 (a) of Durak and Özdemir. [36], Akman *et al*. [38], and the weighted average values (Fig. 8(b)), with our own semi theoretical calculation of the $I_{L\gamma}/I_{L\alpha}$ intensity ratio, computed using Equation (1) across elements with atomic numbers ranging from $_{36}$Kr to $_{92}$U, at an incident photon energy of 59.54keV. Our calculations show a close match with the results reported by Kumar *et al*. [18], with relative deviation (*RD*) ranging from 0% to 7.49% except for $_{40}$Zr, which shows a deviation of (10.73%). Additionally, the data align well with the measurements of Durak and Özdemir [36], with agreement in the lanthanides ($57 \leq Z \leq 72$) ranging from 0.16% to 8.96%, although deviations of 6-37.93% are observed for heavier elements ($74 \leq Z \leq 92$). When compared to the experimental results documented by Akman *et al*. [38], the agreement is within 0.11-8.12% for most elements, except for two outliers $_{70}$Yb (12.98%) and $_{73}$Ta (13.29%). For Demir and Sahin. [39], discrepancies are found within the range 7.09-12.83% except for $_{82}$Pb, $_{83}$Bi, and $_{90}$Th. Regarding the weighted average values presented in Fig. 8 (b), the agreement is generally within 0.25-9.98%, with some exceptions.

To summarize, while the semi-theoretical intensity ratios demonstrate strong agreement with theoretical calculations across a broad range of elements, discrepancies with experimental data, particularly for heavier elements, highlight the inherent challenges in the experimental determination of X-ray intensity ratios for such elements. The results indicate the need for further refinement in experimental techniques, especially heavy elements, to achieve closer alignment with theoretical models.

6. Conclusion

In conclusion, the semi-theoretical $I_{L\beta}/I_{L\alpha}$ and $I_{L\gamma}/I_{L\alpha}$ intensity ratios, derived from the analytical adjustments based on theoretical data from Kumar *et al*. [18], demonstrate a strong ability to predict intensity ratios for elements in the range $36 \leq Z \leq 92$ across various photon energies. The three-dimensional interpolation model, accounting for both atomic number Z and incident photon energy E, shows the robustness of the semi-theoretical approach. Comparisons with experimental data from the literature further validate the precision of the model, particularly in the lower energy regions. While discrepancies at higher energies are noted, the semi-theoretical values are found to be highly consistent with theoretical predictions across the majority of the examined range. This suggests that the semi-theoretical method offers a valuable tool for X-ray fluorescence analysis, providing accurate and reliable intensity ratio estimates. Future work could focus on addressing the few discrepancies at higher photon energies to enhance the model's applicability in a broader energy spectrum.

7. Acknowledgements

We gratefully acknowledge the support of the DGRSDT, Ministry of Higher Education and Scientific Research, Algeria. This work was done with the support of Mohamed El Bachir El Ibrahimi University, under project (PRFU) N°: B00L02UN340120230004. This work was also supported by the Fundação para a Ciência e Tecnologia (FCT), Portugal through contracts UIDP/50007/2020 (LIP) and UID/FIS/04559/2020 (LIBPhys). S.C. warmly acknowledges the financial support of Lancaster University, and A.F. gratefully acknowledges the support of the Joint Research Centre of the European Commission.

Figure caption:

Fig. 1. The distribution of the theoretical $I_{L\beta}/I_{L\alpha}$ intensity ratio as a function of atomic number Z and photon energies below the K-edge. The interpolation result is also presented as a surface.

Fig. 2. The distribution of the theoretical $I_{L\beta}/I_{L\alpha}$ intensity ratio as a function of atomic number Z and photon energies above the K-edge. The interpolation result is also presented as a surface.

Fig. 3. The distribution of the theoretical $I_{L\gamma}/I_{L\alpha}$ intensity ratio as a function of atomic number Z and photon energies below the K-edge. The interpolation result is also presented as a surface.

Fig. 4. The distribution of the theoretical $I_{L\gamma}/I_{L\alpha}$ intensity ratio as a function of atomic number Z and photon energies above the K-edge. The interpolation result is also presented as a surface.

Fig. 5. Comparison of the present semi-theoretical $I_{L\beta}/I_{L\alpha}$ intensity ratio with theoretical, experimental, and weighted average values as a function of atomic number Z at an incident energy of 22.6keV.

Fig. 6. Comparison of the present semi-theoretical $I_{L\beta}/I_{L\alpha}$ intensity ratio with theoretical, experimental, and weighted average values as a function of atomic number Z at an incident energy of 59.54keV.

Fig. 7. Comparison of the present semi-theoretical $I_{L\gamma}/I_{L\alpha}$ intensity ratio with theoretical, experimental, and weighted average values as a function of atomic number Z at an incident energy of 22.6keV.

Fig. 8. Comparison of the present semi-theoretical $I_{L\gamma}/I_{L\alpha}$ intensity ratio with theoretical, experimental, and weighted average values as a function of atomic number Z at an incident energy of 59.54keV.

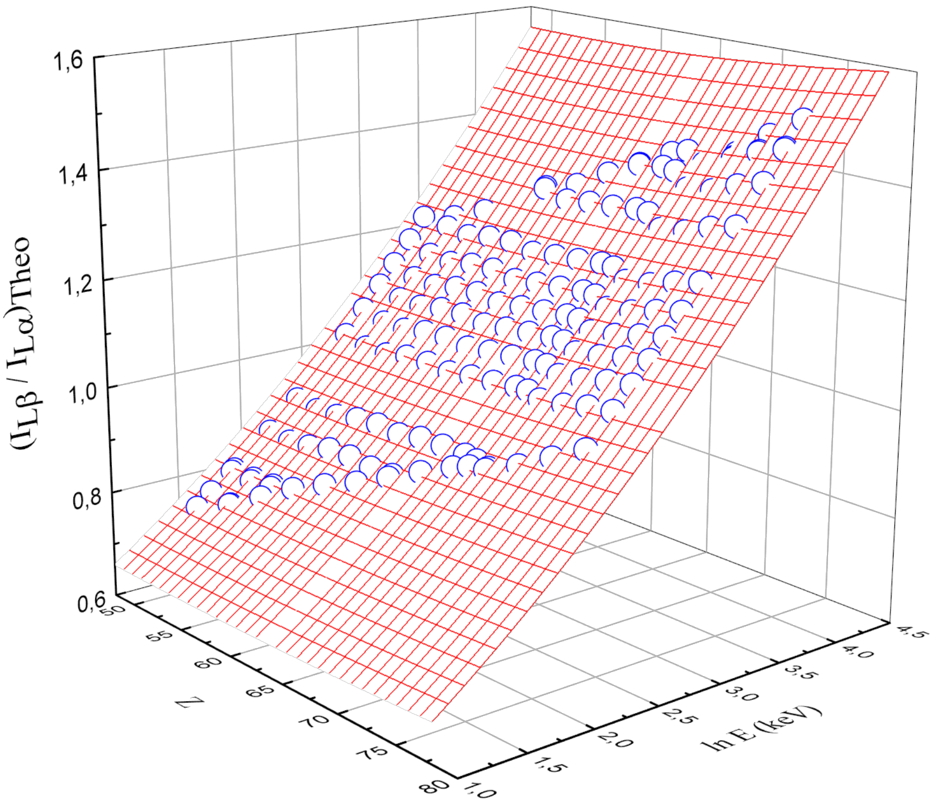

1,6
1,4
1,2
1,0
0,8
0,6
(ILβ / ILα)Theo
50
55
60
65
70
75
80
Z
1,0
1,5
2,0
2,5
3,0
3,5
4,0
4,5
ln E (keV)

Fig.1

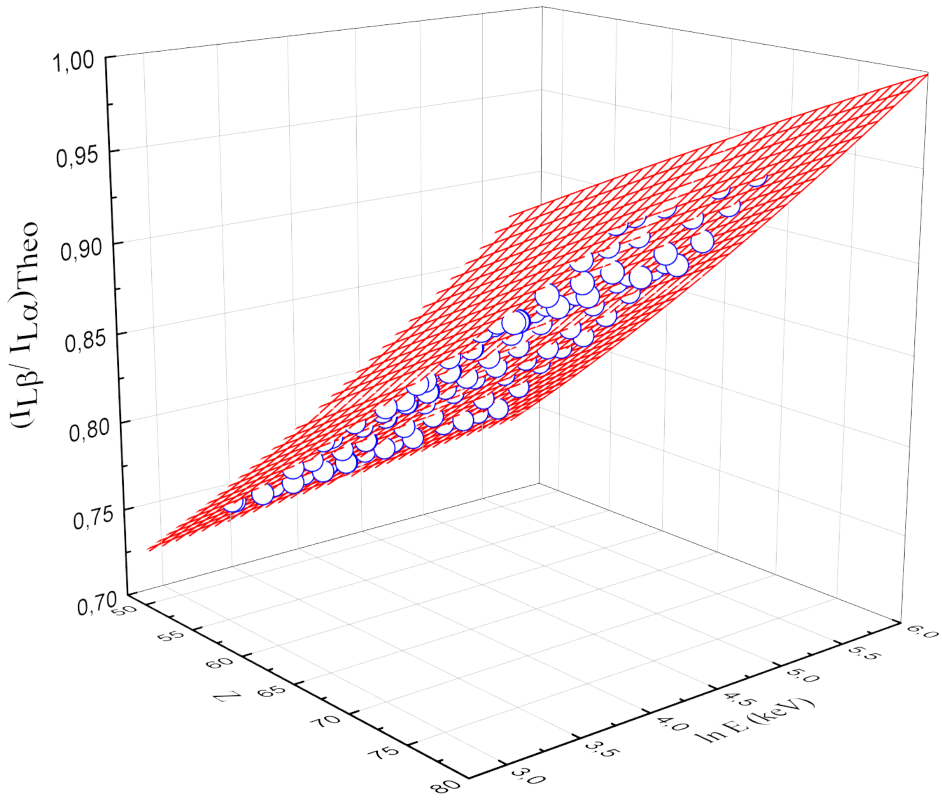

1,00
0,95
0,90
0,85
0,80
0,75
0,70
(ILβ/ ILα)Theo
50
55
60
65
70
75
80
Z
3,0
3,5
4,0
4,5
5,0
5,5
6,0
ln E (keV)

Fig.2

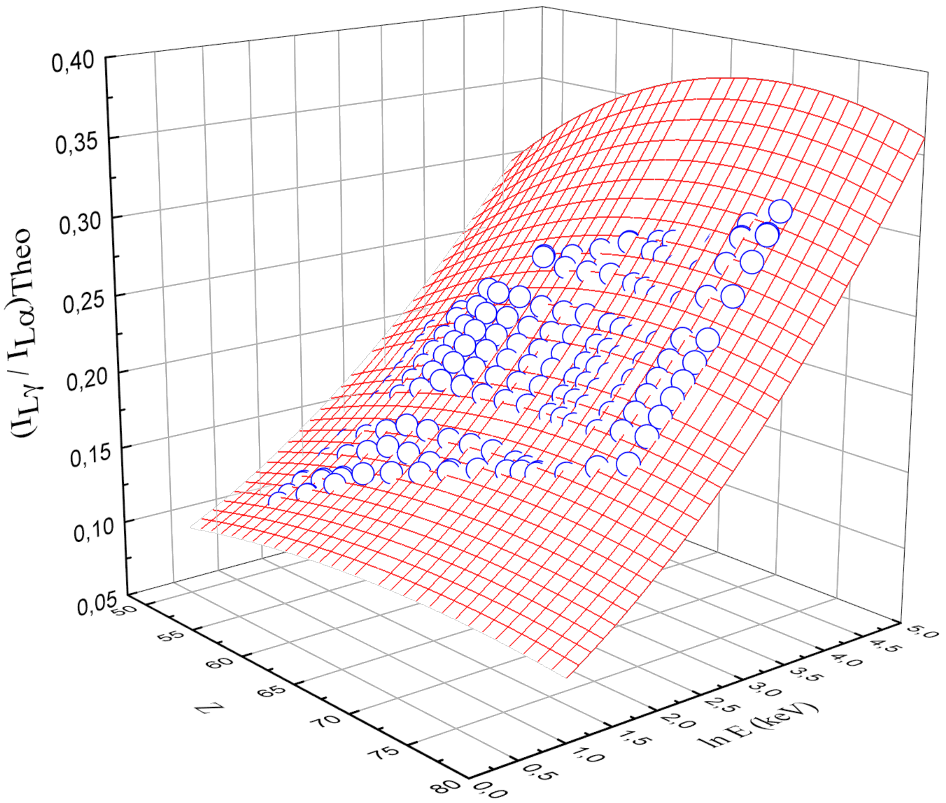

0,40
0,35
0,30
0,25
0,20
0,15
0,10
0,05
$(I_{L\gamma} / I_{L\alpha})$Theo
50
55
60
65
70
75
80
Z
0,0
0,5
1,0
1,5
2,0
2,5
3,0
3,5
4,0
4,5
5,0
ln E (keV)

Fig.3

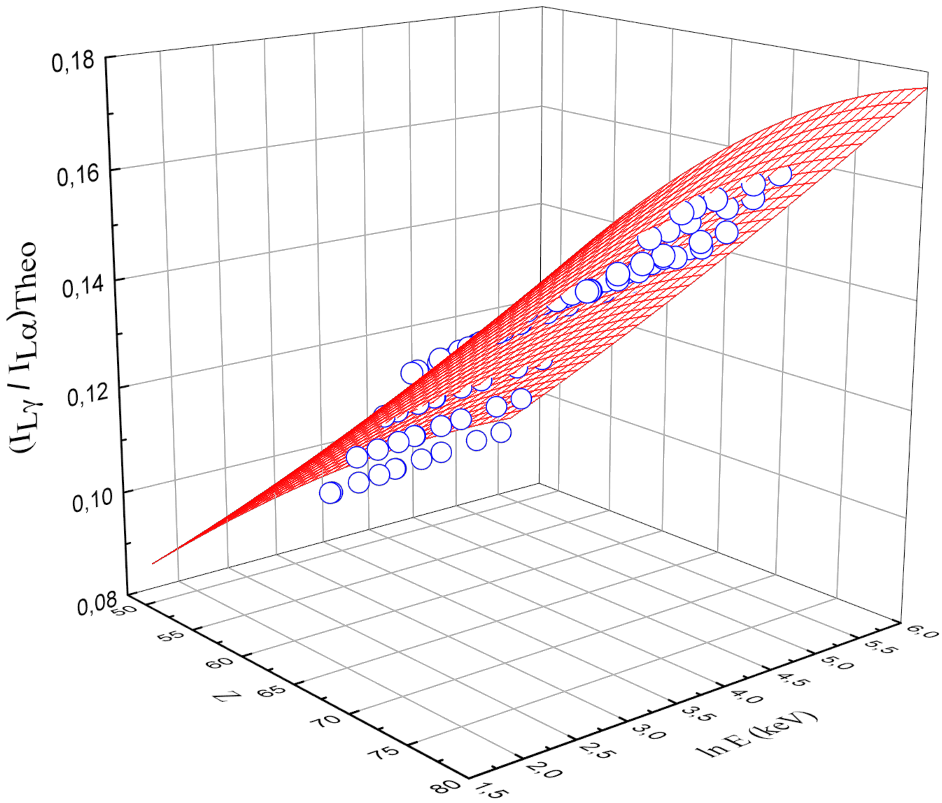

0,18
0,16
0,14
0,12
0,10
0,08
$(I_{L\gamma} / I_{L\alpha})$Theo
50
55
60
65
70
75
80
Z
1,5
2,0
2,5
3,0
3,5
4,0
4,5
5,0
5,5
6,0
ln E (keV)

Fig.4

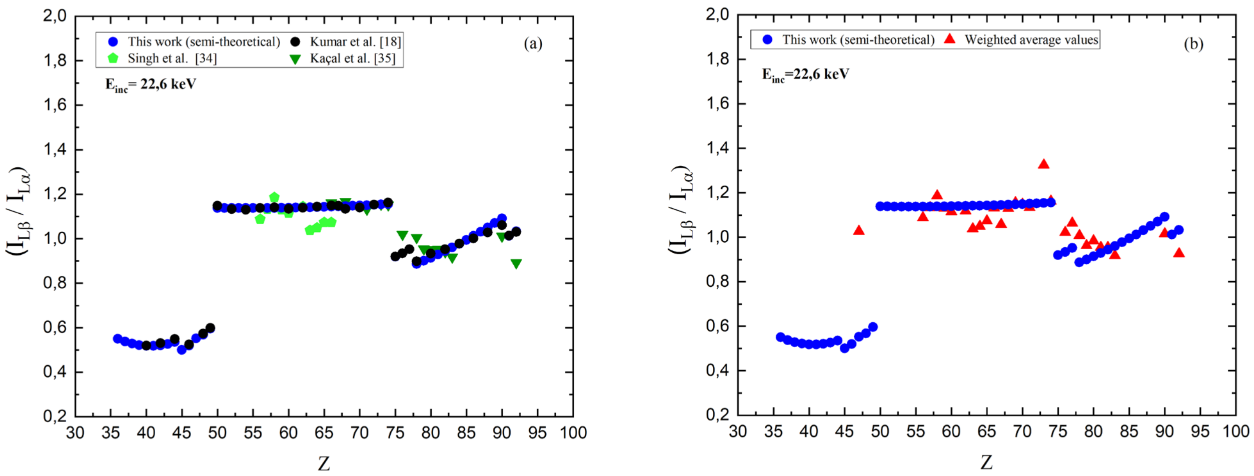

(a)
This work (semi-theoretical)
Kumar et al. [18]
Singh et al. [34]
Kaçal et al. [35]
E_inc= 22,6 keV
(I_Lβ / I_Lα)
Z
(b)
This work (semi-theoretical)
Weighted average values
E_inc=22,6 keV
(I_Lβ / I_Lα)
Z

Fig.5

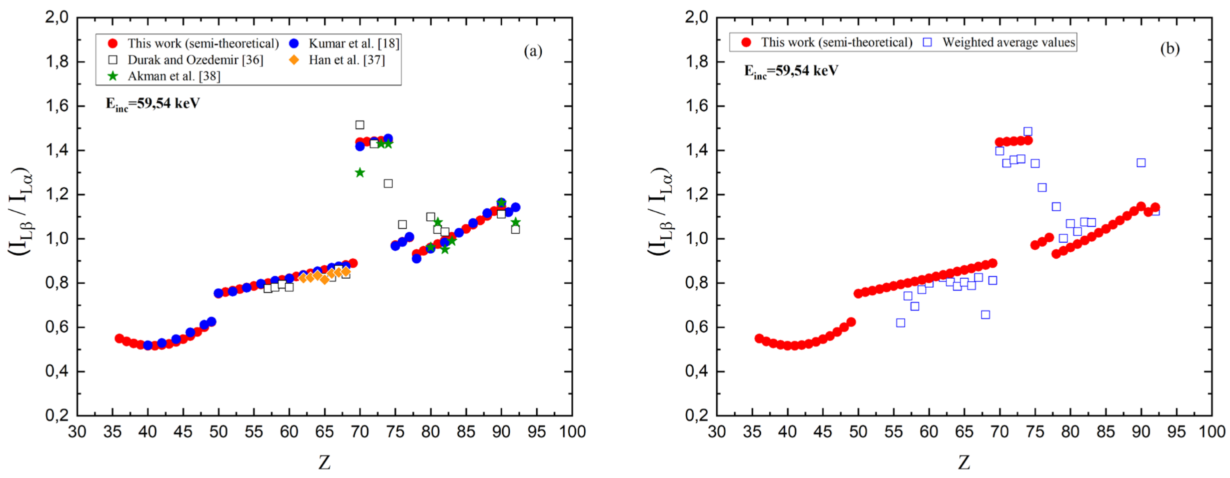

This work (semi-theoretical)
Kumar et al. [18]
Durak and Ozedemir [36]
Han et al. [37]
Akman et al. [38]
(a)
E_{inc}=59,54 keV
$(I_{L\beta} / I_{L\alpha})$
Z
This work (semi-theoretical)
Weighted average values
(b)
E_{inc}=59,54 keV
$(I_{L\beta} / I_{L\alpha})$
Z

Fig. 6

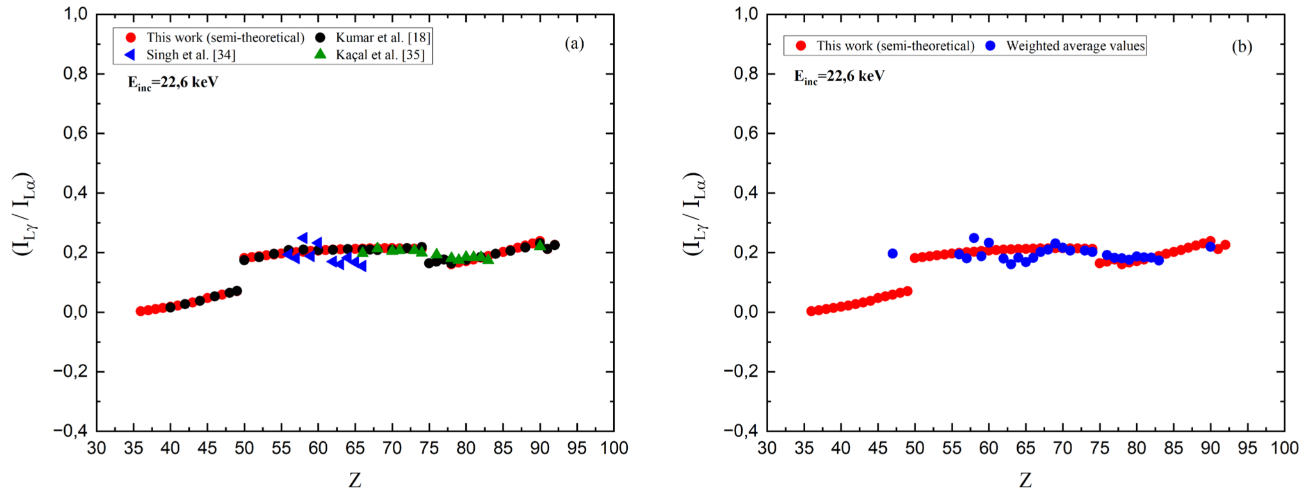

This work (semi-theoretical)
Kumar et al. [18]
Singh et al. [34]
Kaçal et al. [35]
(a)
E_inc=22,6 keV
(I_Lγ / I_Lα)
Z
This work (semi-theoretical)
Weighted average values
(b)
E_inc=22,6 keV
(I_Lγ / I_Lα)
Z

Fig. 7

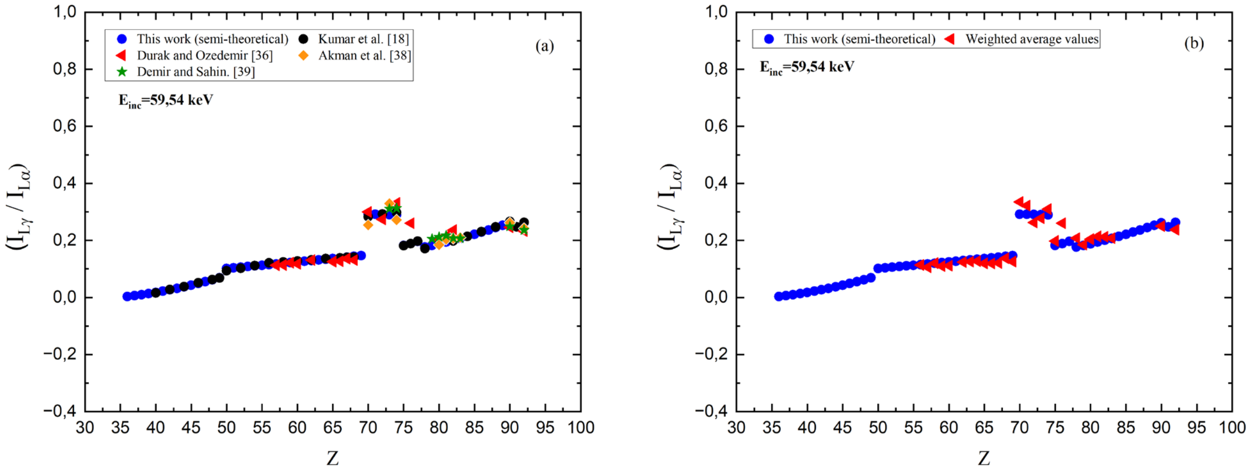
(a)
This work (semi-theoretical)
Kumar et al. [18]
Durak and Ozedemir [36]
Akman et al. [38]
Demir and Sahin. [39]
E_{inc}=59,54 keV
$(I_{L\gamma} / I_{L\alpha})$
Z
(b)
This work (semi-theoretical)
Weighted average values
E_{inc}=59,54 keV
$(I_{L\gamma} / I_{L\alpha})$
Z

Fig. 8

References

[1] K. Amari, A. Kahoul, J.M. Sampaio, Y. Kasri, J.P. Marques, F. Parente, A. Hamidani, S. Croft, A. Favalli, Y. Kasri, A. Zidi, and B. Berkani, Empirical calculation of K-shell fluorescence cross sections for elements in the atomic range 16 ≤ Z ≤ 92 by photon effects ranging from 5.46 to 123.6 keV (Three-dimensional formulae), Phys. Scripta, 99 (2024) 105402, https://doi.org/10.1016/j.jqsrt.2025.109393.

[2] B. Berkani, A. Kahoul, J.M. Sampaio, S. Daoudi, J.P. Marques, F. Parente, A. Hamidani, S. Croft, A. Favalli, Y. Kasri, A. Zidi, and K. Amari, Vacancy transfer probability parameters: Database and a new empirical value for elements in the atomic number range 16 ≤ Z ≤ 92, Radiat. Phys. Chem., 225 (2024) 112106, https://doi.org/10.1016/j.radphyschem.2024.112106

[3] A. Hamidani, S. Daoudi, A. Kahoul, J.M. Sampaio, J.P. Marques, F. Parente, S. Croft, A. Favalli, N. Kup Aylikci, V. Aylikci, Y. Kasri, K. Meddouh, Updated database, semi-empirical and theoretical calculation of Kβ/Kα intensity ratios for elements ranging from 11Na to 96Cm, At. Data Nucl. Data Tables, 149 (2023) 101549–58, https://doi.org/10.1016/j.adt.2022.101549

[4] K. Meddouh, S. Daoudi, A. Kahoul, J.M. Sampaio, J.P. Marques, F. Parente, N.K. Aylikci, V. Aylikci, Y. Kasri, A. Hamidani, Average K-, L-, and M-shell fluorescence yields: A new semi-empirical formulae, Radiat. Phys. Chem., 202 (2023) 110481, https://doi.org/10.1016/j.radphyschem.2022.110481

[5] Y. Sahnoune, A. Kahoul, Y. Kasri, B. Deghfel, D. E. Medjadi, F. Khalfallah, S. Daoudi, V. Aylikçi, N. Küp Aylikçi, M. Nekkab, L1, L2, and L3 subshell fluorescence yields: Updated database and new empirical values, Radiat. Phys. Chem., 125 (2016) 227–251, https://doi.org/10.1016/j.radphyschem.2016.04.016

[6] Y. Sahnoune, A. Kahoul, S. Daoudi, J. M. Sampaio, N. K. Aylikci, V. Aylikci, Y. Kasri, B. Deghfel, J. P. Marques, D. E. Medjadi, Updated database, new empirical and theoretical values of average L shell fluorescence yields of elements with 23≤Z≤96, Radiat. Phys. Chem., 166 (2020) 108495, https://doi.org/10.1016/j.radphyschem.2019.108495

[7] K. Meddouh, A. Kahoul, J. M. Sampaio, S. Daoudi, J. P. Marques, F. Parente, N. K. Aylikci, V. Aylikci, Y. Kasri, A. Hamidani, Semi-Empirical and Theoretical Calculation of 1, 2, and 3 Subshell Fluorescence Yields, J. Quant. Spectrosc. Radiat. Transf., 322 (2024) 109013, https://doi.org/10.1016/j.jqsrt.2024.109013

[8] E. Cengiz, M. Dogan, O.K. Koksal, LIII subshell absorption jump ratio factor of tantalum, Radiat. Phys. Chem., 85 (2013) 8–11, https://doi.org/10.1016/j.radphyschem.2012.10.010

[9] E. Cengiz, N. Saritas, M. Dogan, O.K. Koksal, K. Karabulut, G. Apaydin, E. Tirasoğlu, Measurement of L_{III} subshell absorption jump parameters of hafnium, Spectroscopy and Spectral Analysis 35(12) (2015), 3544-3548, DOI: 10.3964/j.issn.1000-0593(2015)12-3544-05

[10] E. Cengiz, E. Tıraşoğlu, G. Apaydin, O.K. Koksal, Determination of L-shell fluorescence parameters of thallium in thallium compounds, Spectrosc. Lett., 54(4) (2021) 274-280, https://doi.org/10.1080/00387010.2021.1927108.

[11] M.L. Garg, D. Mehta, H.R. Verma, N. Singh, P.C. Mangal, P.N. Trehan, Measurement of L X-ray fluorescence cross sections and relative intensities for Ho, Er and Yb in the energy range 11-41 keV, J. Phys. B: At. Mol. Phys., 19(11) (1986) 1615-1622, https://doi.org/10.1088/0022-3700/19/11/016.

[12] D. V. Rao, G. E. Gigante, R. Cesareo, L-shell x-ray intensity ratios for Au and Pb at excitation energies 36.82, 43.95, 48.60, 50.20 and 53.50 keV, Physica Scripta, 47(6) (1993) 765–768, https://doi.org/10.1088/0031-8949/47/6/013.

[13] B. Dhal, H. Padhi, Relative L-shell X-ray intensities of Pt, Pb and Bi following ionization by 59.54 keV γ-rays, Nucl. Instrum. Methods Phys. Res. B: Beam Interact. Mater. At., 94(4) (1994) 373-376, https://doi.org/10.1016/0168-583X(94)95410-0

[14] S. I. Salem, S. L. Panossian, and R. A. Krause, Experimental K and L relative x-ray emission rates, At. Data Nucl. Data Tables, 14(2) (1974) 91–109, https://doi.org/10.1016/S0092-640X(74)80017-3

[15] J. H. Scofield, Relativistic Hartree-Slater values for K and L X-ray emission rates, At. Data Nucl. Data Tables, 14(2) (1974a) 121–137, https://doi.org/10.1016/S0092-640X(74)80019-7

[16] J. H. Scofield, Hartree-Fock values of L x-ray emission rates, Phys. Rev. A, 10(5) (1974b) 1507–1510, https://doi.org/10.1103/PhysRevA.10.1507.

[17] S. Puri, Relative intensities for Li (i=1–3) and Mi (i=1–5) subshell X-rays, At. Data Nucl. Data Tables, 93(5) (2007) 730–741, https://doi.org/10.1016/j.adt.2007.05.002

[18] A. Kumar, Y. Chauhan, S. Puri, Incident photon energy and Z dependence of L X-ray relative intensities, At. Data Nucl. Data Tables, 96(6) (2010) 567-585, https://doi.org/10.1016/j.adt.2010.03.001.

[19] S. Puri, X-ray relative intensities at incident photon energies across the Li (*i*=1–3) absorption edges of elements with, At. Data Nucl. Data Tables, 100(4) (2014) 847–858, https://doi.org/10.1016/j.adt.2013.11.006

[20] A. Zidi, A. Kahoul, J.P. Marques, S. Daoudi, J.M. Sampaio, F. Parente, A. Hamidani, S. Croft, A. Favalli, Y. Kasri, K. Amari, and B. Berkani, Databases of L-shell X-ray intensity ratios for various elements after photon excitation, At. Data Nucl. Data Tables, 157 (2024) 101645, https://doi.org/10.1016/j.adt.2024.101645

[21] A. Zidi, A. Kahoul, J.P. Marques, S. Daoudi, J.M. Sampaio, F. Parente, A. Hamidani, S. Croft, A. Favalli, Y. Kasri, K. Amari, and B. Berkani, Investigating empirical and theoretical calculations for intensity ratios of L-Shell X-ray transitions in atoms with 39≤Z≤94, J. Electron Spectrosc. Relat. Phenom., 275 (2024) 147473, https://doi.org/10.1016/j.elspec.2024.147473

[22] J. L. Campbell, Fluorescence yields and Coster–Kronig probabilities for the atomic L subshells, At. Data Nucl. Data Tables, 85(2) (2003), 291-315, https://doi.org/10.1016/S0092-640X(03)00059-7

[23] J. L. Campbell, Fluorescence yields and Coster–Kronig probabilities for the atomic L subshells. Part II: The L1 subshell revisited, At. Data Nucl. Data Tables, 95(1) (2009), 115-124, https://doi.org/10.1016/j.adt.2008.08.002

[24] J. A. Bearden and A. F. Burr, Reevaluation of X-Ray Atomic Energy Levels, Reviews of Modern Physics, 39(1) (1967), 125-142, https://doi.org/10.1103/RevModPhys.39.125

[25] V. Aylikci, A. Kahoul, N. K. Aylikci, E. Tiraşoğlu, İ. H. Karahan, A. Abassi, M. Dogan, Empirical and semi-empirical interpolation of L X-ray fluorescence parameters for elements in the atomic range 50 ≤ Z ≤ 92, Radiat. Phys. Chem., 106 (2015) 99-125, https://doi.org/10.1016/j.radphyschem.2014.06.030.

[26] A. Kahoul, V. Aylikci, N.K. Aylikci, E. Cengiz, G. Apaydın, Updated database and new empirical values for K-shell fluorescence yields, Radiat. Phys. Chem., 81(7) (2012) 713-727, https://doi.org/10.1016/j.radphyschem.2012.03.006

[27] D. Mehta, H. Kaur, M.L. Garg, H.R. Verma, N. Singh, T.S. Cheema, P.N. Trehan, X-ray and gamma ray intensity measurements in 141Ce and 170Tm decays, Nucl. Instrum. Methods Phys. Res. A: Accel. Spectrom. Detect. Assoc. Equip. 242 (1) (1985) 149–152, https://doi.org/10.1016/0168-9002(85)90900-3.

[28] D. Mehta, M.L. Garg, J. Singh, N. Singh, T.S. Cheema, P.N. Trehan, Precision measurements of X and gamma-ray intensities in 192Ir, 160Tb, 169Yb and 152Eu decays, Nucl. Instrum. Methods Phys. Res. A: Accel. Spectrom. Detect. Assoc. Equip. 245 (1986) 447–454, https://doi.org/10.1016/0168-9002(86)91281-7

[29] D. Mehta, S. Singh, H.R. Verma, N. Singh, P.N. Trehan, X-and gamma-ray intensity measurements in 137Cs and 203Hg decays, Nucl. Instrum. Methods Phys. Res. A: Accel. Spectrom. Detect. Assoc. Equip. 254 (1987) 578–582, https://doi.org/10.1016/0168-9002(87)90032-5

[30] D. Mehta, B. Chand, S. Singh, M.L. Garg, N. Singh, T.S. Cheema, P.N. Trehan, X-ray and gammaray intensity measurements in 210Pb, 177Lu, 170Tm and 141Ce decays, Nucl. Instrum. Methods Phys. Res. A: Accel. Spectrom. Detect. Assoc. Equip. 260 (1) (1987) 157–159, https://doi.org/10.1016/0168-9002(87)90398-6

[31] B. Chand, J. Goswamy, D. Mehta, N. Singh, P.N. Trehan, X-ray and gamma-ray intensity measurements in 131I, 166Ho, 198Au and 199Au decays, Nucl. Instrum. Methods Phys. Res. A: Accel. Spectrom. Detect. Assoc. Equip. 284 (1989) 393–398, https://doi.org/10.1016/0168-9002(89)90307-0

[32] B. Chand, J. Goswamy, D. Mehta, N. Singh, P.N. Trehan, Studies on the decays of 153Sm and 153Gd to 153Eu, Int. J. Radiat. Appl. Instrum. Part A. Appl. Radiat. Isot. 43 (8) (1992) 997–1004, https://doi.org/10.1016/0883-2889(92)90218-4.

[33] S. Daoudi, A. Kahoul, N.K. Aylikci, J.M. Sampaio, J.P. Marques, V. Aylikci, B. Deghfel, Review of experimental photon-induced Kβ/Kα intensity ratios, At. Data Nucl. Data Tables 132 (2020) 101308–101340, https://doi.org/10.1016/j.adt.2019.101308.

[34] S. Singh, D. Mehta, M.L. Garg, S. Kumar, N. Singh, P.C. Mangal, P.N. Trehan, Measurement of L X-ray fluorescence cross sections and relative intensities for elements $56 \leqslant Z \leqslant 66$ in the energy range 11-41 keV, J. Phys. B: Atom. Mol. Phys. 20 (20) (1987) 5345–5353, https://doi.org/10.1088/0022-3700/20/20/012.

[35] M.R. Kaçal, R. Durak, F. Akman, M.F. Turhan, I. Han, Measurement of L subshell fluorescence cross sections and intensity ratios of heavy elements at 22.6keV, Radiat. Phys. Chem. 80 (6) (2011) 692–700, https://doi.org/10.1016/j.radphyschem.2011.02.009

[36] R. Durak, Y. Özdemir, Measurement of Lα/Lℓ, Lα/Lβ and Lα/Lγ X-ray intensity ratios for elements in the atomic range 57⩽ Z⩽ 92 using radioisotope X-ray fluorescence, Phys. Lett. A 284 (1) (2001) 43–48, https://doi.org/10.1016/S0375-9601(01)00223-7.

[37] I. Han, M. Şahin, L. Demir, Angular variations of K and L X-ray fluorescence cross sections for some lanthanides, Can. J. Phys. 86 (2) (2008) 361–367, https://doi.org/10.1139/p07-128.

[38] F. Akman, R. Durak, M.R. Kaçal, M.F. Turhan, Measurement of Li X-ray fluorescence production cross sections and intensity ratios of some elements at 59.54 keV, Can. J. Phys. 93 (10) (2015) 1057–1066, https://doi.org/10.1139/cjp-2014-0712

[39] D. Demir, Y. Şahin, The effect of an external magnetic field on L X-ray intensity ratios for elements in the range 73≤ Z ≤92 at 59.54 keV, J. Phys. Soc. Jpn. 76 (11) (2007) 114302, https://doi.org/10.1143/JPSJ.76.114302.

Table 1. The fitting coefficients for the calculation of the semi-theoretical $I_{L\beta}/I_{L\alpha}$ and $I_{L\gamma}/I_{L\alpha}$ intensity ratios for energy range below the K-edge according to the formula (1). The associated root-mean-square errors (ε_{RMS}) are also included.

Intensity ratio	Z-range		a_i, b_i	Values	$\varepsilon_{RMS}(\%)$
$I_{L\beta}/I_{L\alpha}$	$36 \le Z \le 49$	$f(Z)$	a_0	1.69897	0.49
			a_1	−0.07290	
			a_2	0.00094	
		$g(\ln(E))$	b_0	1.67764	
			b_1	−0.02319	
			b_2	− 0.00727	
	$50 \le Z \le 74$	$f(Z)$	a_0	0.92606	0.81
			a_1	− 0.00368	
			a_2	0.00003	
		$g(\ln(E))$	b_0	0.60643	
			b_1	0.16439	
			b_2	0.02657	
	$75 \le Z \le 77$	$f(Z)$	a_0	2.41314	0.025
			a_1	−0.06171	
			a_2	0.00043	
		$g(\ln(E))$	b_0	2.02943	
			b_1	1.15762	
			b_2	−0.12526	
	$78 \le Z \le 90$	$f(Z)$	a_0	1.23423	1.47
			a_1	−0.02529	
			a_2	0.00022	
		$g(\ln(E))$	b_0	1.05043	
			b_1	0.20678	
			b_2	−0.01768	
	$91 \le Z \le 92$	$f(Z)$	a_0	0.97782	0.19
			a_1	−0.02027	
			a_2	0.00017	
		$g(\ln(E))$	b_0	0.26578	
			b_1	0.78518	
			b_2	−0.07940	
$I_{L\gamma}/I_{L\alpha}$	$36 \le Z \le 49$	$f(Z)$	a_0	0.63208	0.19
			a_1	0.12506	
			a_2	−0.00416	
		$g(\ln(E))$	b_0	−0.01222	
			b_1	− 0.00685	
			b_2	0.00120	
	$50 \le Z \le 74$	$f(Z)$	a_0	0.63459	0.5
			a_1	− 0.03702	
			a_2	0.00027	
		$g(\ln(E))$	b_0	−0.09278	
			b_1	−0.04024	
			b_2	−0.01148	

	$75 \leq Z \leq 77$	$f(Z)$	a_0 a_1 a_2	1.47964 -0.03954 0.00027	0.05
		$g(\ln(E))$	b_0 b_1 b_2	0.77075 1.14384 -0.10593	
	$78 \leq Z \leq 90$	$f(Z)$	a_0 a_1 a_2	0.76030 -0.02049 0.00017	0.36
		$g(\ln(E))$	b_0 b_1 b_2	0.36233 0.16816 -0.01297	
	$91 \leq Z \leq 92$	$f(Z)$	a_0 a_1 a_2	0.97766 -0.02735 0.00020	0.039
		$g(\ln(E))$	b_0 b_1 b_2	-0.34086 0.85240 -0.08201	

Table2. The fitting coefficients for the calculation of the semi-theoretical $I_{L\beta}/I_{L\alpha}$and $I_{L\gamma}/I_{L\alpha}$ intensity ratios for energy range above the K-edge according to the formula (1). The associated root-mean-square errors (ε_{RMS}) are also included.

Intensity ratio	**Z-range**		$\boldsymbol{a_i.b_i}$	**Values**	$\boldsymbol{\varepsilon_{RMS}}$**(%)**
$\boldsymbol{I_{L\beta}/I_{L\alpha}}$	$36 \leq Z \leq 49$	$f(Z)$	a_0 a_1 a_2	1.7846 − 0.07290 0.00090	0.59
		$g(\ln(E))$	b_0 b_1 b_2	1.7187 − 0.00512 0.00003	
	$50 \leq Z \leq 74$	$f(Z)$	a_0 a_1 a_2	0.81305 0.00633 0.00005	0.33
		$g(\ln(E))$	b_0 b_1 b_2	0.56433 0.01114 −0.00046	
	$75 \leq Z \leq 77$	$f(Z)$	a_0 a_1 a_2	1.64686 − 0.03732 0.00030	0.061
		$g(\ln(E))$	b_0 b_1 b_2	1.56044 −0.00232 − 0.00004	
	$78 \leq Z \leq 90$	$f(Z)$	a_0 a_1 a_2	0.65019 0.00648 0.00015	0.14
		$g(\ln(E))$	b_0 b_1 b_2	0.42950 −0.00470 0.00026	
	$91 \leq Z \leq 92$	$f(Z)$	a_0 a_1 a_2	0.97787 − 0.01791 0.00024	3.66×10^{-7}
		$g(\ln(E))$	b_0 b_1 b_2	0.75965 0.00010 − 0.00028	
$\boldsymbol{I_{L\gamma}/I_{L\alpha}}$	$36 \leq Z \leq 49$	$f(Z)$	a_0 a_1 a_2	0.60189 −0.04734 0.00086	0.19
		$g(\ln(E))$	b_0 b_1 b_2	0.23326 − 0.01808 0.00204	
	$50 \leq Z \leq 74$	$f(Z)$	a_0 a_1 a_2	0.45859 0.26155 0.00087	0.39
		$g(\ln(E))$	b_0 b_1 b_2	0.00453 0.00075 −0.00007	

	$75 \leq Z \leq 77$	$f(Z)$	a_0 a_1 a_2	1.99861 -0.05356 0.00037	0.003
		$g(\ln(E))$	b_0 b_1 b_2	1.9741 -0.01869 0.00218	
	$78 \leq Z \leq 90$	$f(Z)$	a_0 a_1 a_2	0.45518 $-$ 0.01712 0.00028	0.032
		$g(\ln(E))$	b_0 b_1 b_2	0.18928 -0.00138 0.00006	
	$91 \leq Z \leq 92$	$f(Z)$	a_0 a_1 a_2	.97756 $-$ 0.03197 0.00026	5.97×10^{-9}
		$g(\ln(E))$	b_0 b_1 b_2	0.82502 0.02136 $-$ 0.00235	

Table 3: Semi-theoretical (this work), theoretical, and experimental (other works) $I_{L\beta}/I_{L\alpha}$ X ray intensity ratios by photon effect (22.6 keV) for elements with $36 \leq Z \leq 92$.

Z, Element	Weighted average values	S-Theo (this work)	Kumar *et al.* [18] (theo)	Singh *et al*. [34] (exp)	Kaçal *et al*. [35] (exp)
Z=36, Kr	-	0.5505	-	-	-
Z=37, Rb	-	0.5379	-	-	-
Z=38, Sr	-	0.5284	-	-	-
Z=39, Y	-	0.522	-	-	-
Z=40, Zr	-	0.5186	0.5201	-	-
Z=41, Nb	-	0.5182	-	-	-
Z=42, Mo	-	0.5209	0.5305	-	-
Z=43, Tc	-	0.5267	-	-	-
Z=44, Ru	-	0.5355	0.5488	-	-
Z=45, Rh	-	0.5005	-	-	-
Z=46, Pd	-	0.5202	0.5246	-	-
Z=47, Ag	1.0276	0.5528	-	-	-
Z=48, Cd	-	0.5683	0.5741	-	-
Z=49, In	-	0.5966	0.5993	-	-
Z=50, Sn	-	1.1387	1.1489	-	-
Z=51, Sb	-	1.1383	-	-	-
Z=52, Te	-	1.1381	1.1332	-	-
Z=53, I	-	1.1379	-	-	-
Z=54, Xe	-	1.1378	1.1302	-	-
Z=55, Cs	-	1.1379	-	-	-
Z=56, Ba	1.0880	1.138	1.1385	1.088	-
Z=57, La	1.133	1.1382	-	1.133	-
Z=58, Ce	1.186	1.1385	1.1410	1.186	-
Z=59, Pr	1.131	1.1389	-	1.131	-
Z=60, Nd	1.115	1.1393	1.1341	1.115	-
Z=61, Pm	-	1.1399	-	-	-
Z=62, Sm	1.1189	1.1406	1.1395	1.145	-
Z=63, Eu	1.038	1.1413	-	1.038	-
Z=64, Gd	1.050	1.1422	1.1444	1.050	-
Z=65, Tb	1.074	1.1432	-	1.074	-
Z=66, Dy	1.1325	1.1442	1.1499	1.074	1.161
Z=67, Ho	1.058	1.1453	1.1486	-	-
Z=68, Er	1.130	1.1466	1.1339	-	1.167
Z=69,Tm	1.156	1.1479	-	-	-
Z=70, Yb	1.1479	1.1493	1.1406	-	1.147
Z=71, Lu	1.1343	1.1508	-	-	1.133
Z=72, Hf	-	1.1524	1.1530	-	-
Z=73, Ta	1.3250	1.1541	-	-	1.155
Z=74, W	1.1628	1.1559	1.1631	-	1.152
Z=75, Re	-	0.9193	0.9204	-	-
Z=76, Os	1.0225	0.9341	0.9347	-	1.019
Z=77, Ir	1.064	0.9527	0.9525	-	-
Z=78, Pt	1.0075	0.887	0.8991	-	1.005
Z=79, Au	0.9631	0.9004	-	-	0.954
Z=80, Hg	0.9847	0.9145	0.9329	-	0.951
Z=81, Tl	0.9545	0.9292	-	-	0.953
Z=82, Pb	0.9550	0.9446	0.9532	-	0.941
Z=83, Bi	0.9185	0.9606	-	-	0.918
Z=84, Po	-	0.9773	0.9784	-	-
Z=85, At	-	0.9947	-	-	-
Z=86, Rn	-	1.0127	1.0012	-	-
Z=87, Fr	-	1.0314	-	-	-
Z=88, Ra	-	1.0507	1.0282	-	-
Z=89, Ac	-	1.0708	-	-	-
Z=90, Th	1.0156	1.0914	1.0607	-	1.011
Z=91, Pa	-	1.0127	1.0140	-	-
Z=92, U	0.9258	1.0329	1.0301	-	0.892

Table 4: Semi-theoretical (this work), theoretical, and experimental (other works) $I_{L\gamma}/I_{L\alpha}$ X ray intensity ratios by photon effect (22.6 keV) for elements with $36 \leq Z \leq 92$.

Z, Element	**Weighted average values**	**S-Theo (this work)**	**Kumar *et al.* [18] (theo)**	**Singh *et al.* [34] (exp)**	**Kaçal *et al.* [35] (exp)**
Z=36, Kr	-	0.0035	-	-	-
Z=37, Rb	-	0.0066	-	-	-
Z=38, Sr	-	0.0101	-	-	-
Z=39, Y	-	0.0139	-	-	-
Z=40, Zr	-	0.018	0.0155	-	-
Z=41, Nb	-	0.0224	-	-	-
Z=42, Mo	-	0.0272	0.0272	-	-
Z=43, Tc	-	0.0324	-	-	-
Z=44, Ru	-	0.0379	0.0378	-	-
Z=45, Rh	-	0.0476	-	-	-
Z=46, Pd	-	0.0531	0.0535	-	-
Z=47, Ag	0.1965	0.0589	-	-	-
Z=48, Cd	-	0.0648	0.0647	-	-
Z=49, In	-	0.0709	0.0711	-	-
Z=50, Sn	-	0.1814	0.1741	-	-
Z=51, Sb	-	0.1847	-	-	-
Z=52, Te	-	0.1878	0.1844	-	-
Z=53, I	-	0.1908	-	-	-
Z=54, Xe	-	0.1936	0.1959	-	-
Z=55, Cs	-	0.1962	-	-	-
Z=56, Ba	0.194	0.1987	0.2083	0.194	-
Z=57, La	0.181	0.2010	-	0.181	-
Z=58, Ce	0.249	0.2030	0.2098	0.249	-
Z=59, Pr	0.188	0.2050	-	0.188	-
Z=60, Nd	0.2330	0.2067	0.2081	0.233	-
Z=61, Pm	-	0.2083	-	-	-
Z=62, Sm	0.1803	0.2097	0.2091	0.170	-
Z=63, Eu	0.161	0.2109	-	0.161	-
Z=64, Gd	0.183	0.2119	0.2117	0.183	-
Z=65, Tb	0.168	0.2128	-	0.168	-
Z=66, Dy	0.1827	0.2135	0.2103	0.155	0.198
Z=67, Ho	0.202	0.2140	0.2100	-	-
Z=68, Er	0.2097	0.2143	0.2081	-	0.214
Z=69,Tm	0.231	0.2145	-	-	-
Z=70, Yb	0.2160	0.2145	0.2091	-	0.205
Z=71, Lu	0.2072	0.2143	-	-	0.207
Z=72, Hf	-	0.2139	0.2151	-	-
Z=73, Ta	0.2065	0.2134	-	-	0.207
Z=74, W	0.2018	0.2126	0.2185	-	0.199
Z=75, Re	-	0.1641	0.1641	-	-
Z=76, Os	0.1920	0.1696	0.1697	-	0.193
Z=77, Ir	0.182	0.1770	0.1770	-	-
Z=78, Pt	0.1805	0.1612	0.1640	-	0.181
Z=79, Au	0.1761	0.1663	-	-	0.175
Z=80, Hg	0.1872	0.1716	0.1760	-	0.185
Z=81, Tl	0.1840	0.1771	-	-	0.184
Z=82, Pb	0.1830	0.1829	0.1855	-	0.184
Z=83, Bi	0.1735	0.1890	-	-	0.174
Z=84, Po	-	0.1954	0.1960	-	-
Z=85, At	-	0.2020	-	-	-
Z=86, Rn	-	0.2088	0.2061	-	-
Z=87, Fr	-	0.2160	-	-	-
Z=88, Ra	-	0.2234	0.2175	-	-
Z=89, Ac	-	0.2310	-	-	-
Z=90, Th	0.2195	0.2389	0.2312	-	0.221
Z=91, Pa	-	0.2119	0.2121	-	-
Z=92, U	-	0.2258	0.2252	-	-

Table 5: Semi-theoretical (this work), theoretical, and experimental (other works) $I_{L\beta}/I_{L\alpha}$ X ray intensity ratios by photon effect (59.54 keV) for elements with $36 \leq Z \leq 92$.

Z, Element	**Weighted average values**	**S-Theo (this work)**	**Kumar *et al.* [18] (theo)**	**Durak and Özdemir. [36] (exp)**	**Han *et al.* [37] (exp)**	**Akman *et al.* [38] (exp)**
Z=36, Kr	-	0.5490	-	-	-	-
Z=37, Rb	-	0.5364	-	-	-	-
Z=38, Sr	-	0.5269	-	-	-	-
Z=39, Y	-	0.5205	-	-	-	-
Z=40, Zr	-	0.5171	0.5186	-	-	-
Z=41, Nb	-	0.5168	-	-	-	-
Z=42, Mo	-	0.5195	0.5284	-	-	-
Z=43, Tc	-	0.5252	-	-	-	-
Z=44, Ru	-	0.5340	0.5465	-	-	-
Z=45, Rh	-	0.5458	-	-	-	-
Z=46, Pd	-	0.5607	0.5771	-	-	-
Z=47, Ag	-	0.5787	-	-	-	-
Z=48, Cd	-	0.5997	0.6110	-	-	-
Z=49, In	-	0.6237	0.6257	-	-	-
Z=50, Sn	-	0.7521	0.7542	-	-	-
Z=51, Sb	-	0.7588	-	-	-	-
Z=52, Te	-	0.7656	0.7609	-	-	-
Z=53, I	-	0.7724	-	-	-	-
Z=54, Xe	-	0.7793	0.7786	-	-	-
Z=55, Cs	-	0.7863	-	-	-	-
Z=56, Ba	0.620	0.7933	0.7970	-	-	-
Z=57, La	0.7417	0.8003	-	0.775	-	-
Z=58, Ce	0.6949	0.8074	0.8097	0.781	-	-
Z=59, Pr	0.7694	0.8146	-	0.794	-	-
Z=60, Nd	0.7997	0.8218	0.8204	0.781	-	-
Z=61, Pm	-	0.8291	-	-	-	-
Z=62, Sm	0.8249	0.8365	0.8360	-	0.822	-
Z=63, Eu	0.8048	0.8439	-	-	0.825	-
Z=64, Gd	0.7853	0.8514	0.8531	-	0.834	-
Z=65, Tb	0.8031	0.8589	-	0.826	0.815	-
Z=66, Dy	0.7879	0.8665	0.8697	0.826	0.843	-
Z=67, Ho	0.8253	0.8741	0.8749	0.862	0.848	-
Z=68, Er	0.6569	0.8818	0.8754	0.840	0.852	-
Z=69,Tm	0.812	0.8895	-	-	-	-
Z=70, Yb	1.3970	1.4369	1.4169	1.515	-	1.299
Z=71, Lu	1.342	1.4388	-	-	-	-
Z=72, Hf	1.3563	1.4408	1.4374	1.429	-	-
Z=73, Ta	1.3605	1.4429	-	-	-	1.429
Z=74, W	1.4855	1.4451	1.4526	1.250	-	1.429
Z=75, Re	1.3403	0.9707	0.9675	-	-	-
Z=76, Os	1.2310	0.9863	0.9854	1.064	-	-
Z=77, Ir	-	1.0059	1.0088	-	-	-
Z=78, Pt	1.1448	0.9318	0.9099	-	-	-
Z=79, Au	1.0024	0.9459	-	-	-	-
Z=80, Hg	1.0689	0.9607	0.9547	1.099	-	0.962
Z=81, Tl	1.0327	0.9761	-	1.042	-	1.075
Z=82, Pb	1.0754	0.9923	0.9833	1.031	-	0.952
Z=83, Bi	1.0738	1.0091	-	-	-	0.990
Z=84, Po	-	1.0267	1.0275	-	-	-
Z=85, At	-	1.0449	-	-	-	-
Z=86, Rn	-	1.0639	1.0714	-	-	-
Z=87, Fr	-	1.0835	-	-	-	-
Z=88, Ra	-	1.1038	1.1155	-	-	-
Z=89, Ac	-	1.1248	-	-	-	-
Z=90, Th	1.3435	1.1466	1.1637	1.111	-	1.163
Z=91, Pa	-	1.1204	1.1194	-	-	-
Z=92, U	1.1244	1.1427	1.1427	1.042	-	1.075

Table 6: Semi-theoretical (this work), theoretical, and experimental (other works) $I_{L\gamma}/I_{L\alpha}$ X ray intensity ratios by photon effect (59.54 keV) for elements with $36 \leq Z \leq 92$.

Z,Element	**Weighted average values**	**S-Theo (this work)**	**Kumar *et al*. [18] (theo)**	**Durak and Özdemir. [36] (exp)**	**Akman *et al*. [37] (exp)**	**Demir and Sahin. [39] (exp)**
Z=36, Kr	-	0.0035	-	-	-	-
Z=37, Rb	-	0.0065	-	-	-	-
Z=38, Sr	-	0.0099	-	-	-	-
Z=39, Y	-	0.0136	-	-	-	-
Z=40, Zr	-	0.0177	0.0158	-	-	-
Z=41, Nb	-	0.0221	-	-	-	-
Z=42, Mo	-	0.0268	0.0274	-	-	-
Z=43, Tc	-	0.0319	-	-	-	-
Z=44, Ru	-	0.0372	0.0379	-	-	-
Z=45, Rh	-	0.0430	-	-	-	-
Z=46, Pd	-	0.0490	0.0512	-	-	-
Z=47, Ag	-	0.0554	-	-	-	-
Z=48, Cd	-	0.0621	0.0625	-	-	-
Z=49, In	-	0.0692	0.0678	-	-	-
Z=50, Sn	-	0.1015	0.0939	-	-	-
Z=51, Sb	-	0.1038	-	-	-	-
Z=52, Te	-	0.1060	0.1022	-	-	-
Z=53, I	-	0.1083	-	-	-	-
Z=54, Xe	-	0.1106	0.1115	-	-	-
Z=55, Cs	-	0.1129	-	-	-	-
Z=56, Ba	0.114	0.1152	0.1209	-	-	-
Z=57, La	0.1059	0.1176	-	0.113	-	-
Z=58, Ce	0.1202	0.1199	0.1245	0.114	-	-
Z=59, Pr	0.1100	0.1222	-	0.122	-	-
Z=60, Nd	0.1112	0.1246	0.1275	0.118	-	-
Z=61, Pm	-	0.1270	-	-	-	-
Z=62, Sm	0.1240	0.1293	0.1314	0.131	-	-
Z=63, Eu	0.1253	0.1317	-	-	-	-
Z=64, Gd	0.1273	0.1341	0.1364	-	-	-
Z=65, Tb	0.1194	0.1366	-	0.126	-	-
Z=66, Dy	0.1191	0.1390	0.1390	0.127	-	-
Z=67, Ho	0.1211	0.1414	0.1406	0.136	-	-
Z=68, Er	0.1375	0.1439	0.1412	0.131	-	-
Z=69,Tm	0.126	0.1463	-	-	-	-
Z=70, Yb	0.3345	0.2919	0.2831	0.300	0.254	-
Z=71, Lu	0.322	0.2917	-	-	-	-
Z=72, Hf	0.2628	0.2912	0.2924	0.274	-	-
Z=73, Ta	0.2777	0.2904	-	-	0.329	0.311
Z=74, W	0.3096	0.2894	0.2983	0.331	0.272	0.313
Z=75, Re	0.1979	0.1824	0.1819	-	-	-
Z=76, Os	0.260	0.1885	0.1884	0.260	-	-
Z=77, Ir	-	0.1967	0.1971	-	-	-
Z=78, Pt	0.2077	0.1766	0.1715	-	-	-
Z=79, Au	0.1847	0.1821	-	-	-	0.205
Z=80, Hg	0.2045	0.1879	0.1863	0.203	0.185	0.212
Z=81, Tl	0.2140	0.1940	-	0.214	0.204	0.217
Z=82, Pb	0.2126	0.2004	0.1982	0.236	0.207	0.208
Z=83, Bi	0.2079	0.2070	-	-	0.210	0.207
Z=84, Po	-	0.2140	0.2141	-	-	-
Z=85, At	-	0.2212	-	-	-	-
Z=86, Rn	-	0.2287	0.2304	-	-	-
Z=87, Fr	-	0.2365	-	-	-	-
Z=88, Ra	-	0.2446	0.2471	-	-	-
Z=89, Ac	-	0.2530	-	-	-	-
Z=90, Th	0.2501	0.2617	0.2662	0.246	0.262	0.249
Z=91, Pa	-	0.2472	0.2470	-	-	-
Z=92, U	0.2376	0.2634	0.2634	0.233	0.242	0.236